Running head: Multiscale variation in drought and fire

Multiscale variation in drought controlled historical forest fire activity in the boreal forests of eastern Fennoscandia

Tuomas Aakala[1*], Leena Pasanen[2], Samuli Helama[3], Ville Vakkari[4], Igor Drobyshev[5,6], Heikki Seppä[7], Timo Kuuluvainen[1], Normunds Stivrins[7,8], Tuomo Wallenius[1], Harri Vasander[1], Lasse Holmström[2]

[1]Department of Forest Sciences, P.O. Box 27, FI-00014 University of Helsinki, Finland

[2] Department of Mathematical Sciences, P.O. Box 3000, FI-90014, University of Oulu, Finland

[3]Natural Resources Institute Finland (LUKE), Eteläranta 55, FI-96300 Rovaniemi, Finland

[4]Finnish Meterological Institute, P.O. Box 503, FI-00101 Helsinki, Finland

[5]Sveriges lantbruksuniversitet (SLU), Box 49, 230 53 Alnarp, Sweden

[6]Institut de recherche sur les forêts, Université du Québec en Abitibi-Témiscamingue (UQAT), 445 boul. de l'Université, Rouyn-Noranda, QC J9X 5E4, Canada

[7]Department of Geosciences and Geography, P.O. Box 64, FI-00014 University of Helsinki, Finland

[8]Department of Geography, Faculty of Geography and Earth Sciences, University of Latvia, Riga, Jelgavas street 1, LV-1004, Latvia

*Corresponding author: tuomas.aakala@helsinki.fi, tel +358 50 4486152

Abstract

Forest fires are a key disturbance in boreal forests, and characteristics of fire regimes are among the most important factors explaining the variation in forest structure and species composition. The occurrence of fire is connected with climate, but earlier, mostly local scale studies in the northern European boreal forests have provided little insight into fire-climate relationship before the modern fire suppression period. Here, we compiled annually resolved fire history, temperature and precipitation reconstructions from eastern Fennoscandia from the mid-16th century to the end of the 19th century, a period of strong human influence on fires. We used synchrony of fires over the network of 25 fire history reconstructions as a measure of climatic forcing on fires. We examined the relationship between fire occurrence and climate (summer temperature, precipitation, and a drought index summarizing the influence of variability in temperature and precipitation) across temporal scales, using a scale space multiresolution correlation approach and Bayesian inference that accounts for the annually varying uncertainties in climate reconstructions. At the annual scale, fires were synchronized during summers with low precipitation, and most clearly during drought summers. A scale-derivative analysis revealed that fire synchrony and climate varied at similar, roughly decadal scales. Climatic variables and fire synchrony showed varying correlation strength and credibility, depending on the climate variable and the time period. In particular, precipitation emerged as a credible determinant of fire synchrony also at these time scales, despite the large uncertainties in precipitation reconstruction. The findings explain why fire occurrence can be high during cold periods (such as from mid-17th to early 18th century), and stresses the notion that future fire frequency will likely depend to a greater extent on changes in precipitation than temperature alone. We showed, for the first time, the importance of climate as a decadal-scale driver of forest fires in the European boreal forests,

discernible even during a period of strong human influence on fire occurrence. The fire regime responded both to anomalously dry summers, but also to decadal-scale climate changes, demonstrating how climatic variability has shaped the disturbance regimes in the northern European boreal forests over various time scales.

Keywords: Forest fire; Drought; Fire synchrony, Climate reconstruction; Climate variability; Scale space multiresolution correlation analysis; Scale derivative analysis; Bayesian inference

Introduction

In the boreal zone, fires are a major determinant of forest and landscape structures and dynamics (Goldammer and Furyaev 1996). The occurrence of fires has varied considerably through time and in different regions, due to both natural and anthropogenic causes (Carcaillet et al. 2007, Rogers et al. 2015). Given the longevity of fire effects in northern ecosystems, any changes in fire occurrence impose important long-term effects on forest structure. These include changes in species compositions, tree age-, size, and spatial distributions (Aakala et al. 2009, Wallenius et al. 2010), landscape structure, and biodiversity (Bergeron et al. 2002, Ohlson et al. 2011). Therefore, assessing past patterns, and trends of forest fires and the factors controlling their occurrence is imperative for understanding long-term forest dynamics, but also to anticipate future changes in fire occurrence and the potential feedbacks between climate and fires (Kasischke et al. 1995). Understanding climate-fire relationships in the past is also important for climate modeling, as accurate representation of feedbacks between wildfires and climate is critical for calibrating and testing climate models (Spracklen et al. 2011).

Factors that control the occurrence of fires vary across spatial and temporal scales (Flannigan et al. 2000, Liu et al. 2013). At fine-scales (referred to as bottom-up control) this includes temporal and spatial variation in fuels (amount, condition and distribution), ignition sources, topography, local weather, and barriers to fire spread (Larsen 1997, Kennedy and McKenzie 2010), both due to natural and anthropogenic causes (Zumbrunnen et al. 2012). At larger scales (referred to as top-down regulation), forest fires are controlled by climatic variability (Gedalof 2011, Whitlock et al. 2010, Carcaillet et al. 2002, Marlon et al. 2008). These top-down controls affect fire occurrence in several ways that differ in their time scales; weather influences fire occurrence over short time scales (hourly to daily) by influencing ignitions, at monthly and seasonal time scales by influencing fuel moisture, and at longer time scales by influencing fuel type, abundance, and moisture (Flannigan and Wotton 1991, Flannigan et al. 2000, Larjavaara et al. 2005). There are obvious large geographical gradients in climatic averages that influence fire occurrence (i.e. continental areas burn more frequently than oceanic), but for a given region, climatic variability at various temporal scales is an important cause for variability in fire occurrence (Mayer and Swetnam 2000, Girardin et al. 2009, Trouet et al. 2010, Drobyshev et al. 2016).

Bottom-up and top-down regulations have different consequences for the occurrence of fires, and the forest structures the fires create or modify. Bottom-up regulation leads to variation in timing and spread of fires (Falk et al. 2011), and hence fires occurring independently of one another. As a result, heterogeneity in stand and landscape structures is a ‘signature’ of bottom-up regulation (Swetnam 1993). In contrast, top-down control by climatic variation at interannual to decadal to centennial and longer time scales tends to have the opposite effect by synchronizing fire

93 occurrence over larger spatial scales (Veblen et al. 1999, Drobyshev et al. 2015, Drobyshev et al.
94 2014, Brown 2006).
95
96 In the European boreal forests, numerous studies have shown the historical importance of forest
97 fires on local stand and landscape characteristics (Drobyshev et al. 2014, references in Table 1).
98 Landscape structure (Niklasson and Granström 2000) and anthropogenic influence in the form of
99 ignitions and influence on fire spread (Granström and Niklasson 2008) have been identified as
100 particularly important determinants of fire occurrence and behavior. Although 20th century fire
101 statistics have been shown to be linked with climatic variability at interannual scale in the
102 European boreal forests (Saari 1923, Mäkelä et al. 2012), the role of top-down controls have
103 been variably demonstrated for reconstructions of past fires and has been difficult to disentangle
104 from the human influence (Granström and Niklasson 2008). For instance, for fire occurrence
105 during the past several centuries, Wallenius (2011) found no evidence of links between
106 temperature and the fire cycle. However, recently (Drobyshev et al. 2014) showed that such links
107 were present in Swedish fire history reconstructions, especially evident during the so-called
108 'large fire years' ('fire years' in Zackrisson 1977). During such years weather patterns change
109 the susceptibility of stands to fire at a regional scale leading to synchronized fires over a broad
110 area (Swetnam 1993, Nash and Johnson 1996, Drobyshev et al. 2014).
111
112 Assessing climate-fire relationships over longer time scales contains at least two problematic
113 aspects that need to be considered. First, related to the fire data, it is important to distinguish
114 local scale controls from the influence of large-scale climatic controls (Kennedy and McKenzie
115 2010). This commonly requires widely distributed independent fire history reconstructions

116 (Swetnam and Betancourt 1990, Trouet et al. 2010), or the identification of a threshold in fire
117 sizes which would be indicative of climatically forced events (Drobyshev et al. 2012). Second,
118 related to the methods applied in the analysis of fire-climate relationships, it is possible that the
119 correlation between climate variables and fire occurrence is not constant in time, and this has
120 indeed been demonstrated in North America (Swetnam and Betancourt 1998, Hessl et al. 2004,
121 Gavin et al. 2006). Similarly, if the data contains correlation structures at various time scales, the
122 correlation over short scales might hamper the detection of correlation features over large scales,
123 and vice versa (Grissino-Mayer 1995, Swetnam and Betancourt 1998, Mayer and Swetnam
124 2000).
125
126 In this paper, we examined the relationship between climate and forest fires in eastern
127 Fennoscandia from the mid-16th century to the end of the 19th century to quantify climate
128 controls of regional fire activity at multiple temporal scales and hence the changes in climate
129 forcing upon fire activity. Due to a strong anthropogenic influence on local forest fire regimes
130 during that period, our fire records contained a mixture of climate- and human-related signals
131 (Granström and Niklasson 2008). We therefore focused our analyses on the degree of synchrony
132 in forest fire occurrence across a larger geographic region. In this we assume that synchrony in
133 fire occurrence across sites reflects the degree of climatic forcing upon fire activity (Swetnam
134 1993, Falk et al. 2007, 2011, Heyerdahl et al. 2008); although humans have influenced fire
135 regimes we assume that this influence was local, and owing to the relatively sharp gradients in
136 livelihoods (such as the slash-and-burn agriculture; Heikinheimo 1915) and the poorly enforced
137 forest legislation (Hannikainen 1896), any cultural changes are unlikely to result in shifts in fire
138 synchrony over the entire region.

We hypothesized that fire occurrence shows large-scale synchrony, driven by climate anomalies leading to periods of increased fire occurrence at annual and above-annual time scales. For testing the hypothesis, we applied a novel statistical tool, a scale space multiresolution correlation analysis, which allows for non-constant correlations, considers multiple temporal scales simultaneously, and provides Bayesian inference for establishing the credibility of the fire-climate relationships (Pasanen and Holmström 2017). The latter makes it possible to easily incorporate the uncertainties inherent in the climate reconstructions in the analysis.

Material and methods

Study area

The study focused on boreal forests in the eastern parts of the Fennoscandian Shield (henceforth eastern Fennoscandia). Geographically, the area encompasses Finland and the adjacent Russian provinces (Fig. 1). Most of the bedrock in eastern Fennoscandia is made up of Precambrian granites and gneisses, covered by Pleistocene and Holocene sediments, consisting mainly of podzolized moraines. The forested area exhibits relatively modest variation in topography, although the northern parts are characterized by gently rolling hills (fells) with treeless summits.

The main geographical feature influencing the climate in Fennoscandia is its position between the Atlantic Ocean and the Eurasian continent, the eastern parts of Fennoscandia exhibiting a transition between maritime (to the west) and continental (to the east) climates. However, in all parts of the area at least moderate precipitation is recorded throughout the year. The mean temperature of the warmest month (July) ranges from 17.8°C (SD 1.7°C) in the south (Helsinki)

to 14.6°C (1.4°C) in the north (Sodankylä; all climate averages reported here are for the period 1981-2010). The mean temperature of the coldest month (February) varies from -4.7°C (3.8°C) in the south to -12.7°C (4.6°C) in the north. Mean annual precipitation in the same localities was 682 mm (105 mm) in the south to 530 mm (90 mm) in the northeast. Although there is a north-south gradient in average temperatures across our study area, the temporal variations in temperatures are highly correlated. As an example, summer (JJA) temperatures between Sodankylä (67.4ºN, Fig. 1) and Jyväskylä (62.2ºN) correlate well with one another (r = 0.85 for the period 1950-2000).

The main forest-forming tree species in the region include *Pinus sylvestris* L. (Scots pine) and *Picea abies* (L.) Karst. (Norway spruce). Following the Finnish site type classification into barren, xeric, sub-xeric, mesic and herb-rich sites (Cajander 1949), *P. sylvestris* often dominates or is the only tree species in the barren and xeric sites, while *P. abies* dominates the mesic and in particular the herb-rich sites. Both species can dominate the sub-xeric and mesic sites, and their proportion in a stand is largely dependent on the disturbance history (Kuuluvainen and Aakala 2011). In addition, *Betula* spp. (silver birch, pubescent birch) or in rare instances *Populus tremula* L. (aspen) may dominate high elevation and mesic and herb-rich post-disturbance stands. Of the main species, *P. sylvestris*, *Betula* spp., and *P. tremula* are considered early-successional species. *P. abies* is a late-successional species and often recruits under the canopy of the early-successional species.

In the region, the main traditional uses of fire included slash-and-burn agriculture, pasture burning, land-clearing for hunting, and tar production (Wallenius 2011). In addition,

185 unintentional fires were probably caused by campfires, which were commonly left burning. A
186 characteristic feature in the fire occurrence is a sharp decline in forest fires at the end of the 19th
187 century, which can be attributed to the cessation of slash-and-burn cultivation, changes in land-
188 tenure, and to the fact that timber became a valued raw material and thus fire was handled more
189 carefully, greatly reducing the sources of ignitions (Wallenius 2011).
190
191 *Fire history data*
192 A broad range of spatial and temporal observations is necessary to distinguish local fire patterns
193 from regional-scale patterns, and to encompass both high- and low-frequency changes in fire
194 occurrence (Swetnam 1993). For our purposes, we compiled existing, annual resolution forest
195 fire history reconstructions from eastern Fennoscandia (Fig. 1), and complemented them with
196 several unpublished reconstructions (Table 1, Appendix S1). The data consists mostly of tree-
197 ring based fire-scar chronologies, sometimes supplemented with tree age structures (as in Lankia
198 et al. 2012).
199
200 We obtained the fire years directly as original data or, when available, from the publication for a
201 total of 16 different study areas. To increase the number of areas included and the geographical
202 coverage of the data set, we obtained additional data sets by digitizing graphs from nine
203 published studies, in which this data was presented in a readily useable format. This format was
204 commonly a graph depicting the life-span of an individual tree, the active fire-recording period
205 of the tree, and fire dates (see Appendix S1 for examples). The digitizing procedure adds small
206 uncertainty in the data set, but increased the number of areas to a total of 25.
207

208 The collection of fire history reconstructions contained studies that differed greatly in a number
209 of ways, including sampling effort, site selection, and area and time span covered. For instance,
210 some of the studies sampled landscapes systematically (e.g., Haapanen and Siitonen 1978,
211 Wallenius et al. 2010, unpublished studies in Appendix S1), while in some fire scars were
212 actively searched within a certain area and sampled when encountered. This makes measures
213 such as the proportion of trees or sites recording a fire in a certain years poorly comparable. To
214 avoid problems arising from these disparities, we reduced the data in each study to a time series
215 of fire years and non-fire years. This resulted in a loss of information, but we deemed it
216 necessary to make the studies better comparable.
217
218 A second problematic aspect in the data was the geographically uneven distribution. Study area
219 locations were not an objective sample of eastern Fennoscandian landscapes, but their locations
220 have been selected based on varying (unknown) criteria, such as researcher's interest in a
221 specific area, ease of access, or known abundance of fire scars. This was especially evident in
222 North Karelia (areas 4 to 9 in Fig. 1). We considered this problematic, because this
223 geographically unbalanced sampling would potentially give a greater weight to a certain area in
224 which the fires were not necessarily independent of one another. We hence subjectively grouped
225 nearby sites together. This grouping reduced the number of study areas from the original 25 areas
226 to 14 areas (fire groups).
227
228 Using these fire groups, we formed a simple index of fire synchrony (Swetnam 1993). This index
229 was calculated as a proportion of groups with at least one fire out of total number of fire groups
230 that were active each year (i.e. had trees that were recording; Kilgore and Taylor 1979). Fire
231 history reconstructions covered a varying time period, and in our analyses we truncated the series

232 so that we had a minimum of five active groups, starting from 1554. We extended the analysis
233 period until the year 1900.The number of fires was greatly reduced during latter half of the 19th
234 century mainly due to changes in how people handled fire (Wallenius 2011) and hence also the
235 number of fires in our data set dwindled during the 20th century.
236
237 The procedure of grouping individual studies based on their geographical proximity is potentially
238 problematic, as the individual study areas within each group change through time, potentially
239 introducing unquantifiable error and/or bias in the time series of fire synchrony. To test how
240 sensitive the annual fire synchrony time series was to these changes, we conducted a sensitivity
241 analysis in which we randomly removed 1, 3, or 5 individual sites prior to computing the fire
242 synchrony index (Appendix S2). We repeated this 1000 times, and examined the 95%
243 uncertainty intervals for each year of the fire synchrony. High and low values of fire synchrony,
244 as well as the general shape of the time series appeared fairly insensitive to even the removal of 5
245 individual study sites. Hence, we deemed this as a minor uncertainty and did not further consider
246 it in the analyses.
247
248 *Climate data*
249 We included three climate variables associated with forest fires in our analyses: (1) summer
250 temperatures (mean of June, July and August), (2) summer precipitation (precipitation sum for
251 June, July and August), and (3) a simple drought index, constructed as a linear combination of
252 the two other variables (see below). Instrumental climate data is unavailable for the most of our
253 study period and we used reconstructed climate data. For Fennoscandia, multiple annual
254 resolution temperature and precipitation reconstructions exist. These reconstructions have

originally been calibrated with instrumental climate variability using various statistical approaches and not all of them have been published with uncertainty estimates that we needed for the analysis here. For summer temperatures, suitable data with confidence intervals was available (Matskovsky and Helama 2014), compiled as a combination of maximum latewood density reconstructions from northern Fennoscandia, based on two earlier published data-series (Esper et al. 2012, Melvin et al. 2013).

Similar data were not available for precipitation. Hence, we re-calibrated and verified a recently accomplished precipitation reconstructions of past summer climate variability (originally over the past millennium; Helama et al. 2009, Helama 2014), against the instrumental summer (JJA) precipitation sum data from eastern Finland (precipitation data from Mäkelä et al. 2012). The calibration and verification periods were defined by splitting the period common to all data (1908-1993) into two 43-year intervals, 1908-1950 and 1951-1993 (Table 2). These intervals provided the calibration/verification procedure with the early and late periods, respectively. Transfer functions were produced using linear regression over the calibration period (first for 1908-1950) and the Pearson correlation calculated between the instrumental and reconstructed data. Statistics calculated over the verification period (first for 1951-1993) were the Pearson correlation, reduction of error (RE) and coefficient of efficiency (CE) (Fritts 1976, Briffa et al. 1988). For testing the temporal stability of the transfer functions, we carried out a cross-calibration/verification procedure (Gordon 1982, Briffa et al. 1988), using the periods 1951-1993 and 1908-1950 for calibration and verification tests, respectively. Although the R^2 in the predictions was rather low, the statistics RE and CE were positive for both sub-periods indicating real skill in the reconstruction (Fritts et al. 1990, Briffa et al. 1988); Table 2). Hence, we

278 calibrated the final precipitation reconstruction over the common period (1908-1993) and
279 accompanied this reconstruction with confidence intervals determined using a combination of
280 frequency-domain modeling (Ebisuzaki 1997) and Monte Carlo (Efron and Tibshirani 1986)
281 methods, using established algorithms (Macias Fauria et al. 2010, 2012) at 95% thresholds from
282 the autoregressive structure of the residuals of each transfer function. We used these confidence
283 intervals in obtaining the posterior distributions of the climate variables, which we henceforth
284 refer to as reconstruction error.
285
286 Climatic effects of temperature (or precipitation) on fires can be either amplified or dampened by
287 the influence of precipitation (or temperature). To explore and visualize their combined effect,
288 we compiled a simple drought index by standardizing the temperature and precipitation data to a
289 mean of 0, and unit standard deviation, and subtracted standardized precipitation from
290 standardized temperature. High values for this index indicate warm and/or dry conditions, and
291 low values cold and/or wet conditions. We note that as this index is a linear combination of
292 temperature and precipitation, it should be considered simply as a convenience metric for the
293 purpose of visualizing the combined effect of both variables and aiding in the interpretation of
294 the results.
295
296 *Posterior distributions of climate variables*
297 To obtain posterior distributions of the climate variables in Bayesian analysis of the data, we
298 assumed that the observed annual summer temperatures have a Gaussian distribution as follows,

$$y_i = \mu_i + \epsilon_i,$$

299 where i is the index of the year, y_i is the observed summer temperature, μ_i is the true summer

temperature and ϵ_i is the error term, here assumed to be a Gaussian random variable with $\epsilon_i \sim N(0, \sigma_i^2)$. We estimate σ_i^2 from the confidence intervals of each climate time series by calculating the values that correspond to the given confidence intervals on Gaussian random variables (i.e. the reconstruction error defined earlier). We emphasize here that this approach employs the year-specific uncertainty information included in the climate reconstructions. We use an uninformative flat prior distribution for μ_i, thus obtaining a Gaussian posterior

$$\mu_i \sim N(y_i, \sigma_i^2).$$

An identical approach was used to obtain the posterior distribution for summer precipitation. We derived the posterior distribution of the drought index by assuming that the temperature and the precipitation are independent *a priori* and also that their observation errors are independent. The posterior distribution of drought index can therefore be approximated by drawing random samples from the posterior distributions of the summer temperature and precipitation separately, standardizing each sampled temperature and precipitation series, and computing the difference between the standardized samples.

Posterior distribution of fire probability

The number of fire groups experiencing a fire in each year is assumed to have a binomial distribution

$$x_i \sim Bin(N_i, p_i),$$

where x_i is the number of groups experiencing a fire, $N_i$is the number of fire groups, and p_i is the unknown probability of a fire group experiencing a fire in year i. The probabilities of fire groups experiencing a fire constitute the time series $p = (p_i)$. We assume that the probabilities of

a fire group experiencing a fire p_i and p_j for different years are independent and for each p_i we assign a beta distribution prior,

$$p_i \sim Beta(0.111, 1),$$

so that, (a subjectively estimated) *a priori*, $E(p_i) = 0.100$ and $Var(p_i) = 0.043$. The strength of the $Beta(a, b)$ prior relative to the Binomial likelihood function can be evaluated by the equivalent sample size the prior corresponds to, $n = 0.111 + 1 + 1 = 2.111$ (Bolstad 2004). Since for the most of the analysis period the observed number of fires typically exceeds 10, our prior can indeed be considered relatively vague.

With the above prior and likelihood, the posterior distribution is $Beta(x_i + 0.111, N_i - x_i + 1)$. The posterior mean of p_i is therefore

$$E(p_i|x_i) = \frac{x_i + 0.111}{N_i + 1.111}.$$

Detection of large fire years

We used the posterior distribution of the probabilities of a fire group experiencing a fire p_i to detect the years in which this probability was credibly higher than in its neighborhood, using a 100-year sliding time window centered on year *i*. The years *i* for which the posterior probability of p_i being higher than in its 100-year neighborhood were flagged as large fire years (cf. Drobyshev et al. 2014). This was done by drawing a sample of size 10^4 from the posterior distribution of each p_i and finding the years *i* for which the proportion of the sampled p_i's exceeding the posterior mean of the 100-year average was at least 0.9.

341 *Climate vs large fire years*

342 Next we investigated whether the values of the climate variables considered differed credibly
343 between the large fire years and other years. In our Bayesian framework we do this as follows.
344 A sample time series is drawn from the posterior distribution of a climate variable. The mean of
345 this sampled series is found for the large fire years and all other years. This is then repeated for
346 all 10^4 sampled time series producing two samples of size 10^4, a sample of means for large fire
347 years and a sample of means for other years. These two new samples can be considered as
348 approximations for the posterior distributions for the two means. The proportion of sample time
349 series for which the difference between the two means is positive can be used as a statistic that
350 indicates the influence of a climate variable for large fire years. For temperature and drought,
351 values close to 1 would indicate fire prone conditions. For precipitation, such conditions would
352 correspond to values close to zero.
353
354 Besides being conducted within the same analytical framework as the rest of the analyses, this
355 approach (of using the posterior distributions) has the important additional benefit that it
356 implicitly considers the uncertainty associated with the temperature and precipitation
357 reconstructions, which were incorporated already in the posterior distributions of these variables.
358 This is of significance for statistical inference, as the reconstructions have a varying amount of
359 noise, depending on the variable and the year in question.
360
361 *Scale space multiresolution correlation analysis*
362 To assess the dependence of fire synchrony on climate variables over longer time intervals, we
363 used scale space multiresolution correlation analysis, a recently developed statistical method that

aims to discover correlation structures between two time series at different time scales (Pasanen and Holmström 2017). This method addresses two problematic aspects in detecting correlation structures in time series data, namely that the correlation might not be constant in time, and if the data contains correlation structures at various temporal scales, the correlation on small temporal scale might hamper the detection of correlation patterns on large scale, and vice versa.

Scale space multiresolution correlation analysis has two steps. In the first step, the two time series are decomposed into scale-dependent components and, in the second step, the correlation is analyzed between pairs of such components. For the first step, we used the time series decomposition method proposed by (Pasanen et al. 2013). For the second step, the temporal changes in local correlation between pairs of multiresolution components is analyzed using weighted correlation within a sliding time window of varying length. The method also provides Bayesian inference for establishing the credibility of the correlation structures thus found.

Consider a time series $y = [y_1, \ldots, y_n]$, a smoothing operator S_λ and a smoothed time series $S_\lambda y$. Here $\lambda \geq 0$ is a "smoothing parameter" that controls the amount of smoothing in $S_\lambda y$. An example of such a smoothing parameter is the window length of a moving average: the wider the window the smoother the result. Other popular smoothing methods include local linear regression and spline regression (Eubank 1999). The particular smoother used in scale space multiresolution correlation analysis is related to smoothing splines (Green and Silverman 1993), $S_0 y = y$ and, as λ grows to infinity, the smooth $S_\lambda y$ becomes the linear regression line of the time series (for details, see Erästö and Holmström 2012).

In the approach by (Pasanen et al. 2013), a time series was decomposed into additive scale-dependent multiresolution components as follows. Let $0 = \lambda_1 < \lambda_2 < \cdots < \lambda_L \leq \infty$ be an increasing sequence of smoothing levels. Since $S_{\lambda_1} y = S_0 y = y$, a multiresolution decomposition of a time series y is then given by

$$y = \sum_{j=1}^{L-1} (S_{\lambda_j} - S_{\lambda_{j+1}}) y + S_{\lambda_L} y = \sum_{j=1}^{L} z_{j,}$$

where the z_js are the scale-dependent components $z_j = (S_{\lambda_j} - S_{\lambda_{j+1}}) y, j = 1, \ldots, L-1$, and $z_L = S_{\lambda_L} y$.

Careful selection of the smoothing parameter sequence $0 = \lambda_1 < \lambda_2 < \cdots < \lambda_L \leq \infty$ is required for proper extraction of the salient scale-dependent features of a time series. While trial and error approach could be used, we applied the objective approach developed by (Pasanen et al. 2013). In their approach the smoothing parameter sequence is selected by an optimization algorithm as the local minima of the norm of the "scale-derivative" $D_\lambda y = \frac{\partial S_\lambda y}{\partial \ln(\lambda)}$.

Such analysis can be visualized using the so-called scale-derivative map. As an alternative to the optimization method, such a map can also be used to guide a subjective choice of the smoothing parameter. The color of a pixel in the map indicates the value of the scale-derivative for given time and smoothing level. Positive value of the scale-derivative for a time i and smoothing level λ indicates that the value of the smooth at time i increases when the smoothing level λ increases. Therefore the value of the smooth at time i is smaller than the average in its local neighborhood. The negative value can be interpreted analogously. It follows that the scale-dependent components are shown as oscillating bands of colors in the scale-derivative map. For a single

time series, Pasanen et al. (2013) proposed to define the smoothing parameter sequence used in multiresolution decomposition as the local minima of $\left|\left|D_\lambda y\right|\right|$.

The time series considered in the multiresolution analysis can consist of the actual observed data or alternatively it can also be taken to be the random variable that models the unknown underlying truth or its posterior mean (Pasanen et al. 2013). Here, we consider two time series, a climate variable μ and the fire synchrony time series p. Since now two time series are analyzed, a compromise is needed between the multiresolution smoothing levels suggested by the scale-derivatives of p and μ. This could be achieved by visual inspection, selecting the smoothing values so that they are located as closely as possible between oscillating bands of blue and red in the scale-derivative maps of the posterior means of both p and μ. However, as an automatic, data-driven method Pasanen and Holmström (2017) proposed to choose the levels λ_j as the local minima of

$$\frac{||D_\lambda \mu||}{||\mu||} + \frac{||D_\lambda p||}{||p||}. \quad (1)$$

Note that because of the model used for the observed climate data, the posterior mean $\mathrm{E}(\mu|y)$ of μ in fact equals y. Our goal is to decompose the two time series into two components, corresponding to high and low frequency structures. We are interested in the local correlation structures between the low frequency components and regard the high frequency components as noise. It is therefore sufficient to find just one smoothing level that decomposes each the time series into noise and a component that describes larger scale pattern of variability. If several minima are found in (Eq. 1), we choose to use the smoothing parameter value that appeared to be

most appropriate in view of this goal.

After decomposing the two time series into scale-dependent components, we performed the local correlation analysis for the low frequency components, using weighted correlation within a sliding time window of varying length. We use the so-called bi-weight kernel as the weight function (for details, see Pasanen and Holmström 2017). The time horizon considered in the local correlation of p and μ, that is, the width of the sliding window, is controlled by a parameter denoted by σ. For example, when σ =2.0, 50% of the kernel weight falls within a roughly 100 year window. As different time spans may reveal different structures, a range of values of σ is considered to find the salient structures in different scales. The results of multi-scale local correlation analysis are visualized using color maps where the horizontal axis represents the time and the vertical axis represents $\log_{10}(\sigma)$. The color of a pixel at $(t_{k,}, \log_{10}(\sigma))$ represents the local correlation at time point t_k, where the degree of localness is determined by σ. Henceforth we call such an image a correlation map.

The last step of the analysis is to identify which of the structures suggested by the correlation analysis are credible and which are artifacts caused by random error in the data. For a range of window widths σ, Bayesian inference is used for identifying the time intervals with credibly positive or negative correlations. In this, a sample is first drawn from the joint posterior distribution of the climate variable μ and the fire synchrony time series p. We assume that μ and p are independent a priori, and also that ϵ and x are independent. With these assumptions, a sample from the joint posterior distribution of μ and p can be drawn simply from their marginal posterior distributions.

454

455 Second, we obtain the joint posterior distribution of the local correlation coefficients for each σ
456 considered in the analysis. For this, the posterior samples of the time series are first transformed
457 into posterior samples of the low frequency components by smoothing each sampled time series.
458 The smoothing level λ used for this is determined based on the scale-derivatives of the posterior
459 means of μ and p. The sample of low frequency components is then transformed further into a
460 sample of local correlation coefficients.

461

462 Finally, the time intervals and window widths for which correlation is credibly positive or
463 negative are identified using the sample generated from the joint posterior distribution of the
464 correlation coefficients. For this, one could simply identify for each σ the times for which the
465 marginal posterior probability of the correlation being positive or negative exceeds some
466 threshold value $0 < \alpha < 1$. Because such a point-wise inference is bound to result in a large
467 number false positives, we use simultaneous inference over all times and a fixed σ. We apply the
468 simultaneous inference technique of highest pointwise probabilities (HPW), first described in
469 Erästö and Holmström (2012). For a fixed value of σ, denote by w_i the marginal posterior
470 probability of having positive correlation at time i and by b_i the marginal posterior probability
471 of negative correlation at *i.* In case w_i is larger (smaller) than b_i, denote by E_i the event that
472 correlation is positive (negative) at *i* and let $m_i = \max(w_i, b_i)$. HPW is a greedy algorithm
473 where time points i are selected according to their descending order of the marginal posterior
474 probabilities m_i as long as the joint posterior probability of the events E_i at the selected time
475 points is at least α. Here we have used $\alpha = 0.95$. The results are summarized with a credibility
476 version of the correlation map where each pixel is colored either white, black or gray, depending

477 on whether the correlation is credibly positive, negative or neither.
478
479 We note that errors in the original data due to lack of cross-dating or sampling fire scars using
480 increment cores, as well as the digitization procedure may have led to uncertainties and errors of
481 a few years in the fire dates, which were of concern for the interannual analyses. We suspected
482 that this has likely led to "smearing" of the time series, as some scars formed during years with
483 high fire synchrony may have been assigned to years preceding or following the actual year. For
484 the low-frequency analysis, such errors have less influence, as the analyzed series were
485 smoothed.
486
487 **Results**
488 Fire synchrony, i.e. the proportion of fire groups that recorded a fire in a particular year among
489 all active sites, varied from 0 to 0.6. Our method for detecting large fire years (at 90% credibility
490 level) resulted in 20 occurrences (Fig. 2).
491
492 We hypothesized that these years with exceptionally high fire synchrony would differ
493 climatically from other years so that conditions are more conducive to fires: they are warmer,
494 have less precipitation, and as a linear transformation of the two, have a higher drought index
495 value. The results were consistent with our hypotheses especially for precipitation and the
496 drought index (Fig. 3). For temperature, the differences were less clear but the direction of the
497 deviation from mean summer temperature was still consistent with our expectations.
498
499 For the analysis of climate-fire correlations over longer time-scales, our first step was to identify

500 the smoothing parameter for optimal extraction of the scale-dependent features in each time
501 series. For this, we identified the local minima of the sum of the scaled norms of the scale-
502 derivative (Eq. 1), using the posterior mean for each of the climate time series and the fire
503 synchrony time series. For variables other than the temperature, this analysis yielded multiple
504 candidates for the smoothing parameter λ (Fig. 4 and Fig. 5). However, $\lambda \sim 10^4$ was consistently
505 identified as a local minima for all series (range: $10^{3.9}$ to $10^{4.0}$), i.e. the same smoothing
506 parameter was objectively selected for each of the climate reconstructions. We thus used $\lambda \sim 10^4$
507 as our smoothing parameter in all later analyses. Also, from a visual inspection of the scale-
508 derivative maps, it appears that $\lambda \sim 10^4$ seems to be the smoothing parameter value that best
509 divides the features in the data into small and large scale. The effective size of the smoothing
510 window is then approximately 50 years.
511
512 Following the selection of the optimal smoothing parameter, we ran the scale space
513 multiresolution correlation analyses between the fire synchrony time series and each of the
514 climate variables. As hypothesized, and consistent with the analysis of large fire years, for
515 temperature the smoothed time series (Fig. 6, upper panel) tended to be positively correlated with
516 fire synchrony over long time intervals (Fig 6, middle panel; Pearson correlation over the whole
517 period=0.21). The two time series behaved similarly especially after the early 18th century, as
518 suggested by a credible positive correlation (Fig. 6, lower panel) (maximum correlation=0.76).
519 However, the temporal scale of the analysis expressed as the kernel width (shown as the
520 horizontal width between the black and yellow curves in Fig. 6 middle and lower panels,
521 respectively) greatly influenced the results. Over short time window lengths, correlation between
522 the two series changed between negative and strongly positive (correlation fluctuates from -0.51

523 to 0.85). However, of these short time-scale correlations, only the strongly positive correlations
524 around 1750 and after 1850 were credible.
525
526 For precipitation, the scale-correlation maps (Fig. 7 middle panel) show a negative correlation
527 throughout the entire period analyzed. Compared to temperature, correlations with precipitation
528 were stronger and more credible. There was a large difference especially over long time scales:
529 over the entire analysis period, there was a credible negative correlation (Pearson correlation
530 over the whole period= -0.53) between summer precipitation and fire synchrony. Over short
531 window lengths, these correlations are much more sporadic, especially at the very end of the
532 analysis period showing a strong positive correlation after 1870s.
533
534 Correlation between fire synchrony and the drought index was consistent with the hypothesized
535 direction (Fig. 8). Similar to precipitation (however, with an opposite sign), there was
536 consistently credible correlation on longer temporal scales (Pearson correlation over the whole
537 period=0.60). With shorter kernel widths, the strength of the correlation varied and was the
538 strongest around 1750s (maximum correlation 0.96). At shorter kernel widths there were also
539 spurious (and not-credible) negative correlations. All in all, of the three climatic variables, the
540 correlation between fire synchrony and drought was the strongest.
541
542 **Discussion**
543 Earlier studies in eastern Fennoscandia have often emphasized the role of humans in igniting
544 fires and other bottom-up controls for historical forest fire occurrence (Wallenius 2011). We
545 used a widely-dispersed network of annually resolved fire history reconstructions to reduce the

546 influence of stochasticity in fire occurrence on our results and to increase the climatic signal. We
547 showed that climatic variability was an important (top-down) control of fire synchrony, even
548 during a time period characterized by highly fire-conducive culture and livelihoods (see also
549 Zumbrunnen et al. 2009, Trouet et al. 2010). Importantly, using independent climate
550 reconstructions and the Bayesian analysis framework, we found that these fire-climate linkages
551 were also present and credible at decadal temporal scales, in addition to the more commonly
552 studied interannual scale.
553
554 Over the eastern Fennoscandian region, fire synchrony varied greatly between the years. The
555 cultural practices during the period analyzed (1554-1900) promoted fires, but there were also
556 relatively sharp gradients in livelihoods within the region. For instance, the slash-and-burn
557 agriculture was predominantly practiced in the southeastern parts, but was almost absent in the
558 northern parts and the coastal areas (Heikinheimo 1915). If bottom-up controls drove fire
559 occurrence, we would have expected more or less random fire occurrence (Kellogg et al. 2008)
560 among the different localities. However, the time series of fire occurrence showed distinct peaks,
561 indicating years with highly synchronized fire activity, which we termed large fire years (cf.
562 Drobyshev et al. 2014). Such fire synchrony over large distances (i.e., over hundreds of
563 kilometers) has been used as an indicator of climatic forcing on fire occurrence (Swetnam 1993,
564 Drobyshev et al. 2014, Trouet et al. 2010).
565
566 When analyzing climatic conditions during the large fire years, it was evident that climate
567 imposed a top-down control on fire synchrony: although these years tended to be only slightly
568 warmer than other years, they had clearly less summer precipitation, and were clearly drier than

other years as indicated by the drought index. Hence, out of the two independently reconstructed variables temperature and precipitation, precipitation appeared as a much more important predictor of fire synchrony than temperature. Their combination into a simple drought index was useful in illustrating the joint effect of temperature and precipitation, as the correlations with the drought index were higher and more credible than with either of the two variables alone. The significance of drought as a determinant of forest fire occurrence was not altogether surprising, as it has been documented from modern forest fire statistics in the boreal forests (Larsen and MacDonald 1995, Mäkelä et al. 2012) and elsewhere (e.g., Zumbrunnen et al. 2009, Frejaville et al. 2016). However, in the boreal forests, these relationships are rarely demonstrated prior to the modern era with accurate fire statistics. This is probably due to the rarity of precipitation reconstructions, and the overriding influence of local-scale, bottom-up controls upon fire histories developed within single landscapes.

Fire synchrony at the interannual scale has been shown in a number of studies, particularly in North America (e.g., Swetnam 1993). To our knowledge there is only one previous study reporting fire synchrony over the last several centuries from the European boreal forests (Drobyshev et al. 2014), although Zackrisson (1977) also lists regional, ‘notorious fire years’ from northern Sweden. The large fire years identified in this study were largely dissimilar to the large fire years documented by Drobyshev et al. (2014) from the western parts of Fennoscandia: out of the 20 large fire years detected in our analyses, only two (1666, 1677) were shared between the western and eastern parts of Fennoscandia. However, considering that Fennoscandia lies in a coastal zone between the Atlantic Ocean in the west and the Eurasian interior in the east it is not altogether surprising that the large fire years do not match, as is also visible in the spatial

592 distribution of past droughts in Europe (Cook et al. 2015). Thus, the scarcity of common large
593 fire years is above all an indication that conditions are only rarely susceptible for widely-spread
594 fires over all of Fennoscandia at the same time. The notorious fire years listed by Zackrisson
595 (1977) from northern Sweden agree more frequently with our findings. This agreement is good
596 especially in the 1830s, which in our data set had multiple large fire years (1832, 1835, 1838 and
597 1839), suggesting that fire occurrence in the northernmost parts of Sweden was more closely
598 coupled with eastern Fennoscandia than the rest of the western Fennoscandia (Drobyshev et al.
599 2014).
600
601 In addition to the interannual variability, the scale-derivative maps showed variability in fires at
602 approximately decadal time scales. In our analyses, fire synchrony was highest during the latter
603 half of the 17th century, and from the early 18th century onwards, before the well-documented
604 decline at the end of the 19th century (Wallenius 2011). Low-frequency variability in fire
605 occurrence in the boreal zone is well known from sediment charcoal analyses over the millennial
606 time scales (Carcaillet et al. 2001, 2007, Power et al. 2008), but this variability in fire occurrence
607 has not previously been documented at decadal temporal scales.
608
609 The prevalence of either climate or human activities as a driving force behind fire synchrony has
610 been a subject of much debate in Europe (Niklasson and Granström 2000, Carcaillet et al. 2007,
611 Zumbrunnen et al. 2009), and elsewhere (e.g., Chuvieco et al. 2008). In our analyses, two related
612 lines of evidence pointed to the importance of climate as a source of the detected decadal-scale
613 variability in fire synchrony. First, the scale-derivative analyses detected similar fluctuations at
614 approx. decadal scales when analyzing temperature and fire synchrony, precipitation and fire

synchrony, as well as the drought index and fire synchrony. Second, the correlation analyses over longer time windows showed credibly positive correlation with the drought index, and negative correlations with summer precipitation. Correlations were generally weaker between temperatures and fire synchrony, similar to the results from the annual-scale analysis. The greater role of precipitation also explains why Wallenius (2011) did not find any relationship between area burnt and temperature prior to 20th century. The credibility of the relationship between fire synchrony and summer precipitation was particularly interesting, given that the precipitation reconstruction contains more noise compared to the temperature reconstruction (originating from the uncertainty in the calibration; Matskovsky and Helama 2014). Even when these higher uncertainties in the precipitation reconstruction were taken into account, the correlations were clearly more credible compared to the temperature reconstructions.

The time window width and its location influenced the correlations detected, demonstrating the time dependence of climate-fire correlations (Trouet et al. 2010, Zumbrunnen et al. 2009). For precipitation and drought the correlations were credible throughout the analysis period, except for the shortest analysis windows. In addition, at the end of the 19th century correlations between fire synchrony and all climate variables over short time windows switch from positive to negative (for temperature and drought) or from negative to positive (for precipitation). This change coincides with the drastic reduction of fire occurrence in the region (Wallenius 2011), attributed to changes in land tenure and livelihoods: slash-and-burn agriculture gradually phased out (Heikinheimo 1915), timber itself became a commodity, and changes in land tenure meant that the people had an incentive to prevent their valuable timber from burning. These socio-cultural changes were also concomitant with the beginning of fire suppression activities,

638 although it is unlikely that they were very effective in the agrarian society of the 19th century
639 eastern Fennoscandia (Wallenius 2011). These changes reduced fire occurrence and thus likely
640 effectively decoupled the climate-fire linkages in the tree ring based fire history reconstructions.
641 In the more comprehensive fire statistics starting from the late 19th century these climate
642 connections remain discernible (Saari 1923, Mäkelä et al. 2012). We thus suspect that the
643 credible correlations detected over short time scales at the end of the analysis period are probably
644 coincidental, not causal.
645
646 The results from both the interannual and the decadal scale analyses presented here point to the
647 greater role of precipitation compared to temperature, and this finding is consistent with several
648 earlier studies from the boreal forests. In boreal Europe, using regime-shift detection and area
649 annually burned in two different areas in Sweden, Drobyshev et al. (2016) showed that climate
650 caused centennial-scale variability in fire occurrence in western Fennoscandia. In their analysis,
651 the cold periods associated with the so-called Little Ice Age had an increase in fire occurrence,
652 which is further evidence for the stronger controls by precipitation during historical times.
653 Similarly, in western Quebec, Canada, fires were more frequent in the Little Ice Age, and
654 decreased despite warming, potentially due to reduced frequency of drought conditions
655 (Bergeron and Archambault 1993). Jointly, these findings highlight the importance of variability
656 in precipitation over multiple time scales, when predicting future changes in fire occurrence.
657
658 The influence of climate on fire synchrony has implications for understanding and predicting
659 long-term dynamics in forest and landscape structure and composition (Clark 1990). Importantly,
660 northern European boreal forests are characterized by a mixed-severity fire regime, which are

661 known to produce complex landscape patterns (Fulé et al. 2003, Arno et al. 2000). Fire
662 characteristics are partly dependent on the soil characteristics (Zackrisson 1977), and the
663 structure of the landscape (Niklasson and Granström 2000). The consequences of climate-driven
664 changes in fire regimes are different for forests influenced by stand-replacing crown fires and
665 those mainly driven by low-intensity surface fires (Agee 1998, Pennanen 2002).
666
667 In the case of stand-replacing fires that are the dominant type of fire in mesic, spruce-dominated
668 sites (Wallenius et al. 2002, Kuuluvainen and Aakala 2011), fire initiates new successions, and
669 acts a strong determinant for the landscape composition (Turner and Romme 1994). Based on
670 our results, during time periods of low precipitation and the consequently synchronized fire
671 occurrence in eastern Fennoscandia, the proportion of stands in early successional stages would
672 be increased over these large scales, compared to periods of higher precipitation and fewer
673 droughts. This means that the prevalence of even age structures, and species composition
674 characterized by the early successional Scots pine (on xeric sites), and birch (on mesic sites) on
675 the regional scale was historically controlled in part by the low-frequency variability in
676 precipitation. These types of dynamics are well-documented in the North American boreal
677 forests, where stand-replacing fires are common (Bergeron et al. 2002, Brassard et al. 2008).
678
679 While stand-replacing fires have been the dominant type in the Norway spruce dominated, mesic
680 sites, they have historically been much less frequent compared to surface fires on Scots pine
681 dominated sites. On barren and xeric sites, Scots pine is often the only dominant tree species, and
682 the amount of understory biomass that could act as fuels is generally low (Muukkonen and
683 Mäkipää 2006). On those sites the fire-adapted Scots pine often survive fires, and the effects of

684 past fires are most clearly seen as cohort-like age structures (Kuuluvainen and Aakala 2011).
685 Periods of low precipitation, and consequently high fire synchrony would then tend to produce
686 regionally similar age structures in xeric sites dominated by the Scots pine.
687
688 However, the biggest potential for climate variability to impose changes are in the sub-xeric and
689 mesic sites that are often initially (post-fire) dominated by Scots pine, but also suitable for the
690 more nutrient-demanding and drought-sensitive Norway spruce to gradually establish under the
691 Scots pine canopy. When fires occur frequently enough, spruce is killed by the surface fires and
692 the fire-adapted pines maintain their dominant position. However, given sufficiently long fire
693 intervals, spruce will grow into the canopy. In the continued absence of fire, spruce would
694 gradually replace pines as the dominant species or, in the case of fire, lead to stand-replacing
695 fires as the spruce trees with their low-reaching crowns act as ladder fuel. The latter has been
696 demonstrated in connection with changes in fuel availability in North America (e.g., Fulé et al.
697 2003). Hence, during periods characterized by low precipitation and frequent drought conditions
698 these sites would be characterized by a surface fire regime, leading to pine dominance and a
699 cohort age structure, similar to the xeric sites. During time periods characterized by high
700 precipitation and less frequent droughts, these sites would increasingly move to a fire regime
701 dominated by less frequent, but more severe fires, in part driven by the Norway spruce's role as a
702 ladder fuel.
703
704 We thus speculate that these decadal-scale changes in precipitation and drought may lead to
705 regional shifts in habitat properties and forest age and size structure and species composition.
706 Such fire-driven shifts were visible in the low proportion of Norway spruce at the end of the

slash-and-burn era at the early 20th century in southeastern Finland (Heikinheimo 1915). Although in those particular landscapes humans probably played an important role as indirectly determining the species composition, our findings suggest that these types of fluctuations in species composition may have occurred at much larger scales, due to the changing climatic influence on forest fires. This type of a trajectory is nowadays well visible in the conservation areas in the northern part of the study region, where in the absence of fire previously pure Scots pine stands on sub-xeric sites are gradually being invaded by Norway spruce (T. Aakala, unpublished manuscript).

On a more general level, current ecological understanding maintains that the role of disturbances in the northern European boreal forests can be described by a model, which combines the more traditional stand-replacing disturbances and continuous background mortality in old-growth forests ("gap dynamics") with periodical, intermediate-severity disturbances (Fraver et al. 2008, Kuuluvainen 2009). These disturbance dynamics are considered to be controlled primarily by intrinsic, local factors, such as tree age structures, biomass or fuel availability in the stands, the strong role of humans in igniting fires (Wallenius 2011), or the occurrence of sudden climatic events such as droughts (Aakala et al. 2011, Helama et al. 2012). Our results are an important addition to this understanding of European boreal forest dynamics, by demonstrating that the occurrence of these disturbances has also been dependent on large-scale climatic conditions and their fluctuations at decadal time scales.

Conclusions

Using a geographically extensive compilation of annually resolved local fire history

730 reconstructions, summer temperature and precipitation reconstructions as well as a simple
731 drought index, we examined synchrony of forest fires and its climatic drivers over multiple
732 temporal scales. Synchrony of independent fires is a strong indicator of climatic influence on fire
733 regimes and in our analyses this synchrony and its connection to climate were apparent for
734 individual years as well as at decadal scales, as demonstrated, using the Bayesian scale space
735 multiresolution correlation analysis. Out of the climate variables considered, precipitation and
736 drought were credibly stronger determinants of fire synchrony than summer temperatures,
737 despite larger uncertainties in the precipitation reconstruction. These controls have been
738 prevalent during the strong human influence on northern European boreal forests, influencing
739 boreal fires and forest structures until the late 1800s. The stronger control of precipitation
740 explains in general, why fires can be highly synchronized during periods characterized by cold
741 climatic conditions (such as from ~1650 to 1710), and implies that in the changing climate
742 changes in precipitation are likely to carry much stronger impact on fire activity than climate
743 warming on its own, unless suppressed by human interventions. The results further point to
744 climatic variability playing a more prominent role in the dynamics of northern European boreal
745 forests over various temporal scales than what is commonly considered.
746

747 **Acknowledgements**

748 We thank Antti Haapanen, Jesse Valto, Inari Ylläsjärvi, and Rauli Perkiö for providing fire data.
749 We are especially grateful to Parks & Wildlife Finland and Marja Hokkanen for their
750 unpublished fire data. Ari Venäläinen from the Finnish Meteorological Institute provided
751 precipitation data used in the calibration and verification of the precipitation reconstruction. This
752 work was supported by the Academy of Finland (projects. no 276255, 252629, and 275969, and

project. no 288267 for S.H.). V.V. is beneficiary of an AXA Research Fund postdoctoral grant. I.D. was supported by EU consortium PREREAL, Formas grant 239-2014-1866, and NSERC grant (DDG-2015-00026).

Appendix S1. Unpublished fire history reconstructions.

Appendix S2. Sensitivity analysis of the influence of changing number of active fire history reconstructions on fire synchrony.

LITERATURE CITED

Aakala T., T. Kuuluvainen, T. Wallenius, and H. Kauhanen. 2011. Tree mortality episodes in the intact Picea abies-dominated taiga in the Arkhangelsk region of northern European Russia. Journal of Vegetation Science **22**:322-333.

Aakala T., T. Kuuluvainen, T. Wallenius, and H. Kauhanen. 2009. Contrasting patterns of tree mortality in late-successional Picea abies stands in two areas in northern Fennoscandia. Journal of Vegetation Science **20**:1016-1026.

Agee J. K. 1998. The landscape ecology of western forest fire regimes. Northwest Science **72**:24.

Arno S. F., D. J. Parsons, and R. E. Keane. 2000. Mixed-severity fire regimes in the northern Rocky Mountains: consequences of fire exclusion and options for the future. USDA Forest Service Proceedings RMRS-P-15 **5**:225-232.

Bergeron Y., and S. Archambault. 1993. Decreasing frequency of forest fires in the southern boreal zone of Quebec and its relation to global warming since the end of the'Little Ice Age'. The Holocene **3**:255-259.

776 Bergeron Y., A. Leduc, B. D. Harvey, and S. Gauthier. 2002. Natural fire regime: a guide for
777 sustainable management of the Canadian boreal forest. Silva Fennica **36**:81-95.
778 Bolstad W. M. 2004. Introduction to Bayesian Statistics, John Willey & Sons. Inc., New Jersey.
779 Brassard B. W., H. Y. Chen, J. R. Wang, and P. N. Duinker. 2008. Effects of time since stand-
780 replacing fire and overstory composition on live-tree structural diversity in the boreal forest
781 of central Canada. Canadian Journal of Forest Research **38**:52-62.
782 Briffa K. R., P. D. Jones, J. R. Pilcher, and M. K. Hughes. 1988. Reconstructing summer
783 temperatures in northern Fennoscandinavia back to AD 1700 using tree-ring data from Scots
784 pine. Arctic and Alpine Research **20**:385-394.
785 Brown P. M. 2006. Climate effects on fire regimes and tree recruitment in Black Hills ponderosa
786 pine forests. Ecology **87**:2500-2510.
787 Cajander A. K. 1949. Forest types and their significance. Acta Forestalia Fennica **56**:1-71.
788 Carcaillet C., H. Almquist, H. Asnong, R. Bradshaw, J. S. Carrion, M. Gaillard, K. Gajewski, J.
789 N. Haas, S. G. Haberle, and P. Hadorn. 2002. Holocene biomass burning and global
790 dynamics of the carbon cycle. Chemosphere **49**:845-863.
791 Carcaillet C., I. Bergman, S. Delorme, G. Hornberg, and O. Zackrisson. 2007. Long-term fire
792 frequency not linked to prehistoric occupations in northern Swedish boreal forest. Ecology
793 **88**:465-477.
794 Carcaillet C., Y. Bergeron, P. J. Richard, B. Frchette, S. Gauthier, and Y. T. Prairie. 2001.
795 Change of fire frequency in the eastern Canadian boreal forests during the Holocene: does
796 vegetation composition or climate trigger the fire regime? Journal of Ecology **89**:930-946.
797 Chuvieco E., L. Giglio, and C. Justice. 2008. Global characterization of fire activity: toward
798 defining fire regimes from Earth observation data. Global Change Biology **14**:1488-1502.

799 Clark J. S. 1990. Fire and climate change during the last 750 yr in northwestern Minnesota.
800 Ecological Monographs **60**:135-159.
801 Cook E. R., R. Seager, Y. Kushnir, K. R. Briffa, U. Bntgen, D. Frank, P. J. Krusic, W. Tegel, G.
802 van der Schrier, and L. Andreu-Hayles. 2015. Old World megadroughts and pluvials during
803 the Common Era. Science advances **1**:e1500561.
804 Drobyshev I., P. C. Goebel, Y. Bergeron, and R. G. Corace. 2012. Detecting changes in climate
805 forcing on the fire regime of a North American mixed-pine forest: A case study of Seney
806 National Wildlife Refuge, Upper Michigan. Dendrochronologia **30**:137-145.
807 Drobyshev I., Y. Bergeron, H. W. Linderholm, A. Granström, and M. Niklasson. 2015. A 700-
808 year record of large fire years in northern Scandinavia shows large variability and increased
809 frequency during the 1800 s. Journal of Quaternary Science **30**:211-221.
810 Drobyshev I., Y. Bergeron, A. de Vernal, A. Moberg, A. A. Ali, and M. Niklasson. 2016.
811 Atlantic SSTs control regime shifts in forest fire activity of Northern Scandinavia. Scientific
812 reports **6**:22532.
813 Drobyshev I., A. Granström, H. W. Linderholm, E. Hellberg, Y. Bergeron, and M. Niklasson.
814 2014. Multi-century reconstruction of fire activity in Northern European boreal forest
815 suggests differences in regional fire regimes and their sensitivity to climate. Journal of
816 Ecology **102**:738-748.
817 Ebisuzaki W. 1997. A method to estimate the statistical significance of a correlation when the
818 data are serially correlated. Journal of Climate **10**:2147-2153.
819 Efron B., R. Tibshirani. 1986. Bootstrap methods for standard errors, confidence intervals, and
820 other measures of statistical accuracy. Statistical science **1**:54-75.
821 Erästö P., and L. Holmström. 2012. Bayesian multiscale smoothing for making inferences about

features in scatterplots. Journal of Computational and Graphical Statistics **14**:569-589.

Esper J., D. C. Frank, M. Timonen, E. Zorita, R. J. Wilson, J. Luterbacher, S. Holzkmper, N. Fischer, S. Wagner, and D. Nievergelt. 2012. Orbital forcing of tree-ring data. Nature Climate Change **2**:862-866.

Eubank R. L. 1999. Nonparametric regression and spline smoothing. Marcel Dekker, New York.

Falk D. A., C. Miller, D. McKenzie, and A. E. Black. 2007. Cross-scale analysis of fire regimes. Ecosystems **10**:809-823.

Falk D. A., E. K. Heyerdahl, P. M. Brown, C. Farris, P. Z. Fulé, D. McKenzie, T. W. Swetnam, A. H. Taylor, and M. L. Van Horne. 2011. Multi-scale controls of historical forest-fire regimes: new insights from fire-scar networks. Frontiers in Ecology and the Environment **9**:446-454.

Flannigan M. D., and B. M. Wotton. 1991. Lightning-ignited forest fires in northwestern Ontario. Canadian Journal of Forest Research **21**:277-287.

Flannigan M. D., B. J. Stocks, and B. M. Wotton. 2000. Climate change and forest fires. Science of the total environment **262**:221-229.

Fraver S., B. G. Jonsson, M. Jönsson, and P.-A. Esseen 2008. Demographics and disturbance history of a boreal old-growth *Picea abies* forest. Journal of Vegetation Science **19**: 789-798.

Frejaville T., T. Curt, and C. Carcaillet. 2016. Tree cover and seasonal precipitation drive understorey flammability in alpine mountain forests. Journal of Biogeography **43**:1869-1880.

Fritts H. C. 1976. Tree rings and climate. Academic Press, San Fransisco.

Fritts H. C., J. Guiot, G. A. Gordon, and F. Schweingruber. 1990. Methods of calibration,

verification, and reconstruction. Pages 163-217 *In* E. R. Cook and L. A. Kairiukstis, editors. Methods of Dendrochronology - Applications in the Environmental Sciences, Kluwer Academic Press, Boston.

Fulé P. Z., J. E. Crouse, T. A. Heinlein, M. M. Moore, W. W. Covington, and G. Verkamp. 2003. Mixed-severity fire regime in a high-elevation forest of Grand Canyon, Arizona, USA. Landscape Ecology **18**:465-486.

Gavin D. G., F. S. Hu, K. Lertzman, and P. Corbett. 2006. Weak climatic control of stand-scale fire history during the late Holocene. Ecology **87**:1722-1732.

Gedalof Z. 2011. Climate and spatial patterns of wildfire in North America. Pages 89-115 *In* D. McKenzie, C. Miller, and D. A. Falk, editors. The Landscape Ecology of Fire, Springer, Dordrecht.

Girardin, M. P., A. A. Ali, C. Carcaillet, M. Mudelsee, I. Drobyshev, C. Hely, and Y. Bergeron 2009. Heterogeneous response of circumboreal wildfire risk to climate change since the early 1900s. Global Change Biology **15**: 2751-2769.

Goldammer J. G., V. V. Furyaev. 1996. Fire in ecosystems of boreal Eurasia, Springer, Dordrecht.

Gordon G. A. 1982. Verification of dendroclimatic reconstructions. Pages 58-61 *In* M. K. Hugher, P. M. Kelly, J. R. Pilcher, and V. C. LaMarche, editors. Climate from Tree Rings, Cambridge University Press, Cambridge.

Granström A., and M. Niklasson. 2008. Potentials and limitations for human control over historic fire regimes in the boreal forest. Philosophical Transactions of the Royal Society of London B: Biological Sciences **363**:2351-2356.

Green P. J., and B. W. Silverman. 1993. Nonparametric regression and generalized linear

models: a roughness penalty approach. Chapman and Hall, London.

Grissino-Mayer H. D. 1995. Tree-ring reconstructions of climate and fire history at El Malpais National Monument, New Mexico. University of Arizona.

Haapanen A., P. Siitonen. 1978. Forest fires in Ulvinsalo strict nature reserve. Silva Fennica **12**:187-200.

Hannikainen P. W. 1896. Suomen metsät kansallis-omaisuutenamme. Otava, Helsinki. [In Finnish]

Heikinheimo O. 1915. Der Einfluss der Brandwirtschaft auf die Wälder Finnlands. Acta Forestalia Fennica **4**:1-264. [In Finnish with German summary]

Helama S. 2014. The Viking Age as a Period of Contrasting Climatic Trends. *In* J. Ahola, Frog, and C. Tolley, editors. Fibula, Fabula, Fact -- the Viking Age in Finland, Suomalaisen Kirjallisuuden Seura, Helsinki.

Helama S., J. Meriläinen, and H. Tuomenvirta. 2009. Multicentennial megadrought in northern Europe coincided with a global El NioSouthern Oscillation drought pattern during the Medieval Climate Anomaly. Geology **37**:175-178.

Helama S., A. Läänelaid, J. Raisio, and H. Tuomenvirta. 2012. Mortality of urban pines in Helsinki explored using tree rings and climate records. Trees **26**:353-362.

Hessl A. E., D. McKenzie, and R. Schellhaas. 2004. Drought and Pacific Decadal Oscillation linked to fire occurrence in the inland Pacific Northwest. Ecological Applications **14**:425-442.

Heyerdahl E. K., D. McKenzie, L. D. Daniels, A. E. Hessl, J. S. Littell, and N. J. Mantua. 2008. Climate drivers of regionally synchronous fires in the inland Northwest (1651–1900). International Journal of Wildland Fire **17**:40-49.

Kaipainen T. 2001. Metsäpalohistoria Lieksan alueella. M.Sc. thesisUniversity of Helsinki. [In Finnish]

Kärkkäinen J., and M. Nironen. 1997. Oulangan kansallispuiston Uudenniitynsuon luonnonhoitoalueen metsät ja niiden palohistoria. Metsähallituksen luonnonsuojelujulkaisuja, Sarja A **74**. [In Finnish]

Kasischke E. S., N. L. Christensen, and B. J. Stocks. 1995. Fire, global warming, and the carbon balance of boreal forests. Ecological Applications **5**:437-451.

Kellogg L. B., D. McKenzie, D. L. Peterson, and A. E. Hessl. 2008. Spatial models for inferring topographic controls on historical low-severity fire in the eastern Cascade Range of Washington, USA. Landscape Ecology **23**:227-240.

Kennedy M. C., and D. McKenzie. 2010. Using a stochastic model and cross-scale analysis to evaluate controls on historical low-severity fire regimes. Landscape Ecology **25**:1561-1573.

Kilgore B. M., and D. Taylor. 1979. Fire history of a sequoia-mixed conifer forest. Ecology **60**:129-142.

Kuuluvainen T. 2009. Forest management and biodiversity conservation based on natural ecosystem dynamics in northern Europe: the complexity challenge. AMBIO: A Journal of the Human Environment **38**:309-315.

Kuuluvainen T., and T. Aakala. 2011. Natural forest dynamics in boreal Fennoscandia: a review and classification. Silva Fennica **45**:823-841.

Lankia H., T. Wallenius, G. Várkonyi, J. Kouki, and T. Snäll. 2012. Forest fire history, aspen and goat willow in a Fennoscandian old-growth landscape: are current population structures a legacy of historical fires? Journal of Vegetation Science **23**:1159-1169.

Larjavaara M., J. Pennanen, and T. J. Tuomi. 2005. Lightning that ignites forest fires in Finland.

914 Agricultural and Forest Meteorology **132**:171-180.
915 Larsen C. 1997. Spatial and temporal variations in boreal forest fire frequency in northern
916 Alberta. Journal of Biogeography **24**:663-673.
917 Larsen C., and G. M. MacDonald. 1995. Relations between tree-ring widths, climate, and annual
918 area burned in the boreal forest of Alberta. Canadian Journal of Forest Research **25**:1746-
919 1755.
920 Lehtonen H. 1998. Fire history recorded on pine trunks and stumps: influence of land use and
921 fires on forest structure in North Karelia. Scandinavian Journal of Forest Research **13**:462-
922 468.
923 Lehtonen H., and T. Kolström. 2000. Forest fire history in Viena Karelia, Russia. Scandinavian
924 Journal of Forest Research **15**:585-590.
925 Lehtonen H., and P. Huttunen. 1997. History of forest fires in eastern Finland from the fifteenth
926 century AD-the possible effects of slash-and-burn cultivation. The Holocene **7**:223-228.
927 Lehtonen H., P. Huttunen, and P. Zetterberg. 1996. Influence of man on forest fire frequency in
928 North Karelia, Finland, as evidenced by fire scars on Scots pines. Annales Botanici Fennici
929 **33**:257-263.
930 Liu Z., J. Yang, and H. S. He. 2013. Identifying the threshold of dominant controls on fire spread
931 in a boreal forest landscape of northeast China. PloS one **8**:e55618.
932 Macias Fauria M., A. Grinsted, S. Helama, J. Moore, M. Timonen, T. Martma, E. Isaksson, and
933 M. Eronen. 2010. Unprecedented low twentieth century winter sea ice extent in the Western
934 Nordic Seas since AD 1200. Climate Dynamics **34**:781-795.
935 Macias Fauria M., A. Grinsted, S. Helama, and J. Holopainen. 2012. Persistence matters:
936 estimation of the statistical significance of paleoclimatic reconstruction statistics from

937 autocorrelated time series. Dendrochronologia **30**:179-187.
938 Mäkelä H. M., M. Laapas, and A. Venäläinen. 2012. Long-term temporal changes in the
939 occurrence of a high forest fire danger in Finland. Natural Hazards and Earth System
940 Sciences **12**:2591-2601.
941 Marlon J. R., P. J. Bartlein, C. Carcaillet, D. G. Gavin, S. P. Harrison, P. E. Higuera, F. Joos, M.
942 J. Power, and I. C. Prentice. 2008. Climate and human influences on global biomass burning
943 over the past two millennia. Nature Geoscience **1**:697-702.
944 Matskovsky V. V., and S. Helama. 2014. Testing long-term summer temperature reconstruction
945 based on maximum density chronologies obtained by reanalysis of tree-ring data sets from
946 northernmost Sweden and Finland. Climate of the Past **10**:1473-1487.
947 Mayer H. D. G., and T. W. Swetnam. 2000. Century scale climate forcing of fire regimes in the
948 American Southwest. The Holocene **10**:213-220.
949 Melvin T. M., H. Grudd, and K. R. Briffa. 2013. Potential bias in 'updating'tree-ring
950 chronologies using regional curve standardisation: Re-processing 1500 years of Torneträsk
951 density and ring-width data. The Holocene **23**:364-373.
952 Muukkonen P., and R. Mäkipää. 2006. Empirical biomass models of understorey vegetation in
953 boreal forests according to stand and site attributes
954 . Boreal Environment Research **11**:355-369.
955 Nash C. H., and E. A. Johnson. 1996. Synoptic climatology of lightning-caused forest fires in
956 subalpine and boreal forests. Canadian Journal of Forest Research **26**:1859-1874.
957 Niklasson M., A. Granström. 2000. Numbers and sizes of fires: long-term spatially explicit fire
958 history reconstruction in a Swedish boreal landscape. Ecology **81**:1484-1499.
959 Ohlson M., K. J. Brown, H. J. B. Birks, J. Grytnes, G. Hörnberg, M. Niklasson, H. Seppä, and R.

960 H. Bradshaw. 2011. Invasion of Norway spruce diversifies the fire regime in boreal
961 European forests. Journal of Ecology **99**:395-403.
962 Pasanen L., and L. Holmström. 2017. Scale space multiresolution correlation analysis for time
963 series data. Computational Statistics **32**:197.
964 Pasanen L., I. Launonen, and L. Holmström. 2013. A scale space multiresolution method for
965 extraction of time series features. Stat **2**:273-291.
966 Pennanen J. 2002. Forest age distribution under mixed-severity fire regimes-a simulation-based
967 analysis for middle boreal Fennoscandia. Silva Fennica **36**:213-231.
968 Perkiö R. 2003. Metsäpalojen vaikutus haavan (Populus tremula L.) laatuun ja määrään vanhojen
969 metsien suojelualueilla Pohjois-Karjalassa. M.Sc. thesis, University of Joensuu. [In Finnish]
970 Pohjonen R. 2001. Pyhä-Häkin kansallispuiston metsäpalohistoria ja palojen vaikutus puuston
971 rakenteeseen. M.Sc. thesis, University of Joensuu. [In Finnish]
972 Power M. J., J. Marlon, N. Ortiz, P. J. Bartlein, S. P. Harrison, F. E. Mayle, A. Ballouche, R. H.
973 Bradshaw, C. Carcaillet, and C. Cordova. 2008. Changes in fire regimes since the Last
974 Glacial Maximum: an assessment based on a global synthesis and analysis of charcoal data.
975 Climate Dynamics **30**:887-907.
976 Rogers B. M., A. J. Soja, M. L. Goulden, and J. T. Randerson. 2015. Influence of tree species on
977 continental differences in boreal fires and climate feedbacks. Nature Geoscience **8**:228-234.
978 Saari E. 1923. Forest fires in Finland. Acta Forestalia Fennica **26**:1-155.
979 Spracklen D. V., K. S. Carslaw, U. Pschl, A. Rap, and P. M. Forster. 2011. Global cloud
980 condensation nuclei influenced by carbonaceous combustion aerosol. Atmospheric
981 Chemistry and Physics **11**:9067-9087.
982 Swetnam T. W. 1993. Fire history and climate change in giant sequoia groves. Science **262**:885.

983 Swetnam T. W., and J. L. Betancourt. 1998. Mesoscale disturbance and ecological response to
984 decadal climatic variability in the American Southwest. Journal of Climate **11**:3128-3147.
985 Swetnam T. W., and J. L. Betancourt. 1990. Fire-southern oscillation relations in the
986 southwestern United States. Science **249**:1017-1020.
987 Trouet V., A. H. Taylor, E. R. Wahl, C. N. Skinner, and S. L. Stephens. 2010. Fire-climate
988 interactions in the American West since 1400 CE. Geophysical Research Letters **37**:L04702.
989 Turner M. G., W. H. Romme. 1994. Landscape dynamics in crown fire ecosystems. Landscape
990 Ecology **9**:59-77.
991 Veblen T. T., T. Kitzberger, R. Villalba, and J. Donnegan. 1999. Fire history in northern
992 Patagonia: the roles of humans and climatic variation. Ecological Monographs **69**:47-67.
993 Wallenius T. H., H. Kauhanen, H. Herva, and J. Pennanen. 2010a. Long fire cycle in northern
994 boreal Pinus forests in Finnish Lapland. Canadian journal of forest research **40**:2027-2035.
995 Wallenius T. H., H. Kauhanen, H. Herva, and J. Pennanen. 2010b. Long fire cycle in northern
996 boreal Pinus forests in Finnish Lapland. Canadian Journal of Forest Research **40**:2027-2035.
997 Wallenius T. 2011. Major decline in fires in coniferous forests–reconstructing the phenomenon
998 and seeking for the cause. Silva Fennica **45**:1.
999 Wallenius T., T. Kuuluvainen, R. Heikkilä, and T. Lindholm. 2002. Spatial tree age structure and
1000 fire history in two old-growth forests in eastern Fennoscandia. Silva Fennica **36**:185-199.
1001 Wallenius T. H., T. Kuuluvainen, and I. Vanha-Majamaa. 2004. Fire history in relation to site
1002 type and vegetation in Vienansalo wilderness in eastern Fennoscandia, Russia. Canadian
1003 Journal of Forest Research **34**:1400-1409.
1004 Wallenius T. H., A. Pitkänen, T. Kuuluvainen, J. Pennanen, and H. Karttunen. 2005. Fire history
1005 and forest age distribution of an unmanaged Picea abies dominated landscape. Canadian

Journal of Forest Research **35**:1540-1552.

Wallenius T. H., S. Lilja, and T. Kuuluvainen. 2007. Fire history and tree species composition in managed Picea abies stands in southern Finland: implications for restoration. Forest Ecology and Management **250**:89-95.

Whitlock C., P. E. Higuera, D. B. McWethy, and C. E. Briles. 2010. Paleoecological perspectives on fire ecology: revisiting the fire-regime concept. The Open Ecology Journal **3**:6-23.

Zackrisson O. 1977. Influence of forest fires on the North Swedish boreal forest. Oikos **29**:22-32.

Zetterberg P. 1992. Koloveden kansallispuiston metsäpalohistorian dendrokronologinen selvitys. Dendrokronologian laboratorion ajoitusseloste **91**. [In Finnish]

Zumbrunnen T., H. Bugmann, M. Conedera, and M. Bürgi. 2009. Linking forest fire regimes and climate—a historical analysis in a dry inner alpine valley. Ecosystems **12**:73-86.

Zumbrunnen T., P. Menndez, H. Bugmann, M. Conedera, U. Gimmi, and M. Bürgi. 2012. Human impacts on fire occurrence: a case study of hundred years of forest fires in a dry alpine valley in Switzerland. Regional Environmental Change **12**:935-949.

Data Availability Statement

The precipitation reconstruction is available online, DOI: 10.6084/m9.figshare.5357587

1028 **Tables**

1029 **Table 1.** Fire history data sets. Id refers to numbers in Fig. 1.
1030

Id	Area	Fire group	Lat	Lon	Source	Source
1	Evo	Lammi	61.3	25.1	original data	Wallenius et al. 2007
2	Kolovesi	Kolovesi	62.3	28.8	original data	Zetterberg 1992
3	Pyhä-Häkki	Pyhä-Häkki	62.8	25.5	original data	Pohjonen 2001
4	Ahvenjärvi	Northern Karelia	62.9	31.0	digitized	Lehtonen and Huttunen 1997
5	Pönttövaara	Northern Karelia	63.1	31.0	digitized	Lehtonen 1998
6	Autiovaara	Northern Karelia	63.1	30.7	digitized	Lehtonen et al. 1996
7	Salamanperä	Salamanperä	63.2	24.8	original data	Marja Hokkanen, unpubl., see Appendix S1
8	Kitsi	Northern Karelia	63.3	30.8	digitized	Lehtonen and Huttunen 1997
9	Lieksa	Northern Karelia	63.3	30.5	digitized	Kaipainen 2001
10	Pohjois-Karjala	Northern Karelia	63.3	30.6	digitized	Perkiö 2003
11	Teeri-Lososuo	Teeri-Lososuo	63.9	29.3	original data	Lankia et al. 2012
12	Ulvinsalo	Ulvinsalo	64.0	30.4	original data	Haapanen and Siitonen 1978
13	Venehjärvi	Kalevala	65.0	30.2	original data	Wallenius et al. 2004
14	Venehlampi	Kalevala	65.0	30.1	digitized	Lehtonen and Kolström 2000
15	Uudenniitynsuo	Kuusamo	66.4	29.4	original data	Kärkkäinen and Nironen 1997
16	Paanajärvi	Kuusamo	66.5	30.2	original data	Wallenius et al. 2005
17	Maltio	Maltio	67.4	28.7	original data	This study, see Appendix S1
18	Pallas-Ylläs	Pallas-Ylläs	67.7	24.4	original data	Inari Ylläsjärvi, unpubl., see Appendix 1
19	Värriö II	Värriö	67.7	29.5	original data	This study, see Appendix S1
20	Värriö I	Värriö	67.8	29.6	original data	This study, see Appendix S1
21	Kazkim	Kazkim	68.3	30.3	original data	This study, see Appendix S1
22	Saariselkä	Saariselkä	68.4	28.4	original data	Wallenius et al. 2010
23	Talasvaara	Saariselkä	68.8	28.4	original data	Wallenius et al. 2010
24	Kessi II	Saariselkä	68.9	28.4	original data	Jesse Valto, unpublished, see Appendix S1
25	Kessi	Saariselkä	69.0	28.4	original data	Wallenius et al. 2010

1031
1032

Table 2. Calibration and verification statistics for the precipitation reconstruction. The common period (1908-1993) is divided into two sub-periods for cross-validation. Each column shows the R^2 for a given calibration period, followed by the statistics for the verification period. The final reconstruction was calibrated for the entire common period.

Calibration			
Calibration period	1908-1950	1951-1993	1908-1993
R^2	0.298	0.249	0.261
Verification			
Verification period	1951-1993	1908-1950	
R^2	0.062	0.089	
RE	0.043	0.054	
CE	0.043	0.053	

Figure captions

Fig. 1. Study area locations, where neighboring symbols of same color belong to the same 'fire group', i.e. studies that were grouped for the analyses. Numbers in the map refer to Table 1.

Fig. 2. Time series of fire synchrony (posterior mean), the detected exceptional large fire years and the number of active groups.

Fig. 3. Large fire years vs. climate; the posterior distributions of temperature (test statistic 0.88), precipitation (0.00) and drought index (1.00) for the large fire years and other years. The test statistic gives the proportion of sample time series for which the difference between the two means is positive; for temperature (a) and drought (c), values close to 1 would indicate fire prone conditions. For precipitation (b), such conditions would correspond to values close to zero.

Fig. 4. Scale-derivative maps for posterior means of temperature (a), precipitation (b), drought (c) and fire synchrony (d). Black lines indicate the smoothing parameters corresponding to the local minima of (Eq.1; Fig. 5). The local minima for fire synchrony (d) are obtained from Eq. 1, using drought as the climate variable y (hence, the location is the same as with (c)). Deep red corresponds to a large positive value, deep blue to a large negative value, while green indicates a value close to zero.

Fig. 5. The sum of the scaled norms of the scale-derivatives of the posterior means (Eq. 1) for drought (a), precipitation (b) and temperature (c). Black diamonds indicate the locations of local minima and are visualized as black lines in Fig. 4.

Fig. 6. The results of the scale-correlation analysis of smoothed fire synchrony vs. summer temperature reconstruction. The upper panel shows the smoothed time series analyzed (posterior mean values; red = fire synchrony, black = summer temperature). The middle panel shows the correlation map (posterior mean values), and the lower panel the results of the credibility analysis for the correlation map (white = credibly positive correlation, gray = correlation not credible). The horizontal space between the solid lines in the two lower panels indicate the width of a centrally positioned kernel and the dashed lines similarly indicate the width of the interval where the kernel height has decreased to 50% of its maximum value.

Fig. 7. The results of the scale-correlation analysis of smoothed fire synchrony vs. summer precipitation reconstruction. The upper panel shows the smoothed time series analyzed (posterior mean values; red = fire synchrony, black = summer precipitation). The middle panel shows the correlation map (posterior mean values), and the lower panel the results of the credibility analysis for the correlation map (white = credibly positive correlation, gray = correlation not credible, black = credibly negative correlation). Interpretation otherwise as in Fig. 6.

Fig. 8. The results of the scale-correlation analysis of smoothed fire synchrony vs. summer drought index reconstruction. The upper panel shows the smoothed time series analyzed (posterior mean values; red = fire synchrony, black = summer drought index). The middle panel shows the correlation map (posterior mean values), and the lower panel the results of the credibility analysis for the correlation map. Interpretation otherwise as in Fig. 6.

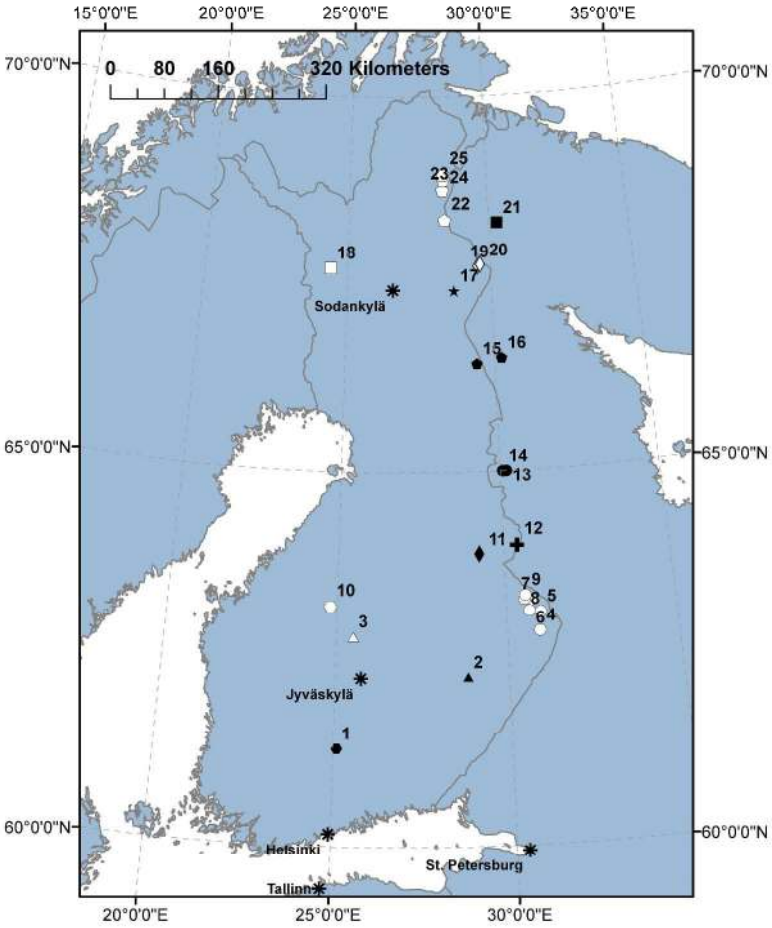

Fig. 1. Study area locations, where neighboring symbols of same color belong to the same 'fire group', i.e. studies that were grouped for the analyses. Numbers in the map refer to Table 1.

296x419mm (300 x 300 DPI)

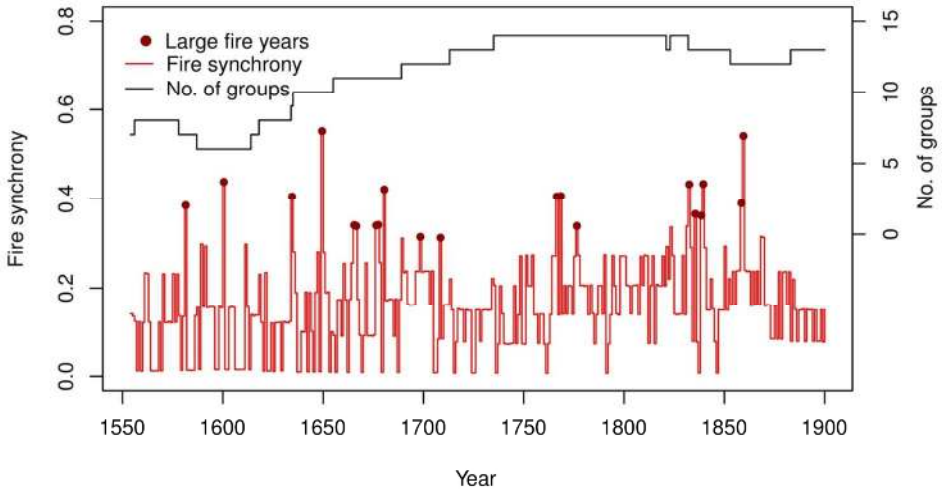

Fig. 2. Time series of fire synchrony (posterior mean), the detected exceptional large fire years and the number of active groups.

128x81mm (300 x 300 DPI)

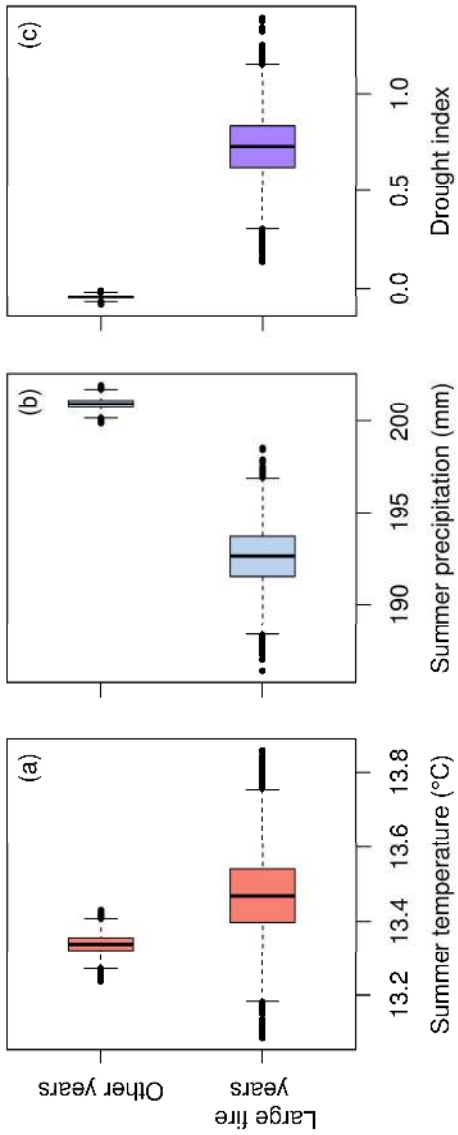

Fig. 3. Large fire years vs. climate; the posterior distributions of temperature (test statistic 0.88), precipitation (0.00) and drought index (1.00) for the large fire years and other years. The test statistic gives the proportion of sample time series for which the difference between the two means is positive; for temperature (a) and drought (c), values close to 1 would indicate fire prone conditions. For precipitation (b), such conditions would correspond to values close to zero.

279x361mm (300 x 300 DPI)

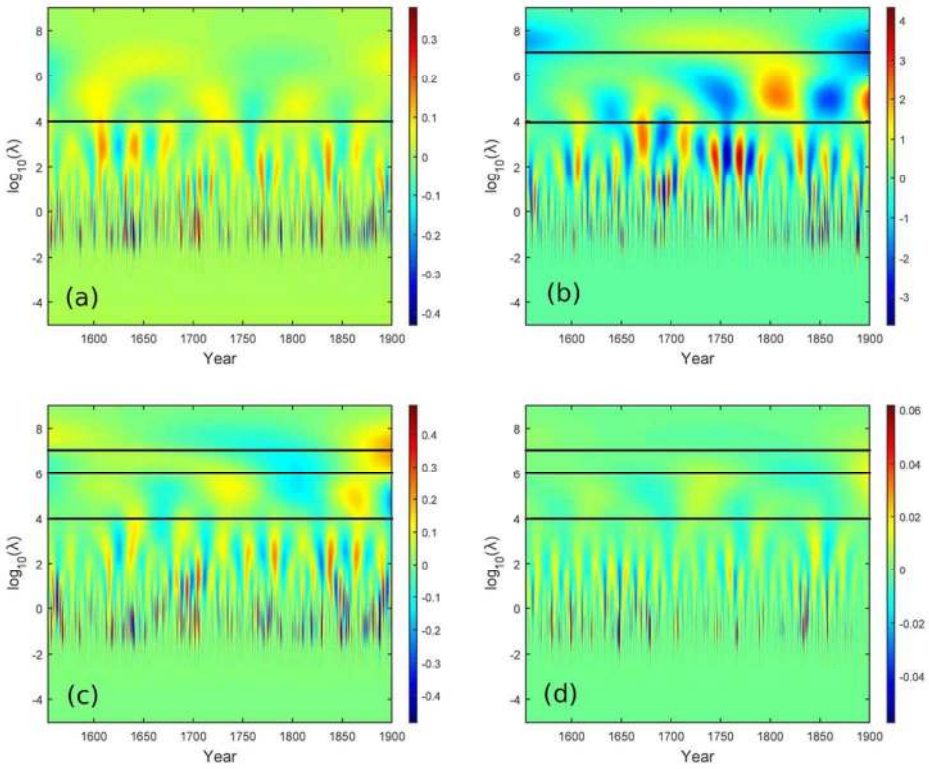

Fig. 4. Scale-derivative maps for posterior means of temperature (a), precipitation (b), drought (c) and fire synchrony (d). Black lines indicate the smoothing parameters corresponding to the local minima of (Eq.1; Fig. 5). The local minima for fire synchrony (d) are obtained from Eq. 1, using drought as the climate variable y (hence, the location is the same as with (c)). Deep red corresponds to a large positive value, deep blue to a large negative value, while green indicates a value close to zero.

101x80mm (300 x 300 DPI)

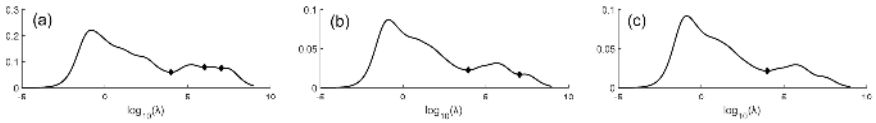

Fig. 5. The sum of the scaled norms of the scale-derivatives of the posterior means (Eq. 1) for drought (a), precipitation (b) and temperature (c). Black diamonds indicate the locations of local minima and are visualized as black lines in Fig. 4.

215x166mm (300 x 300 DPI)

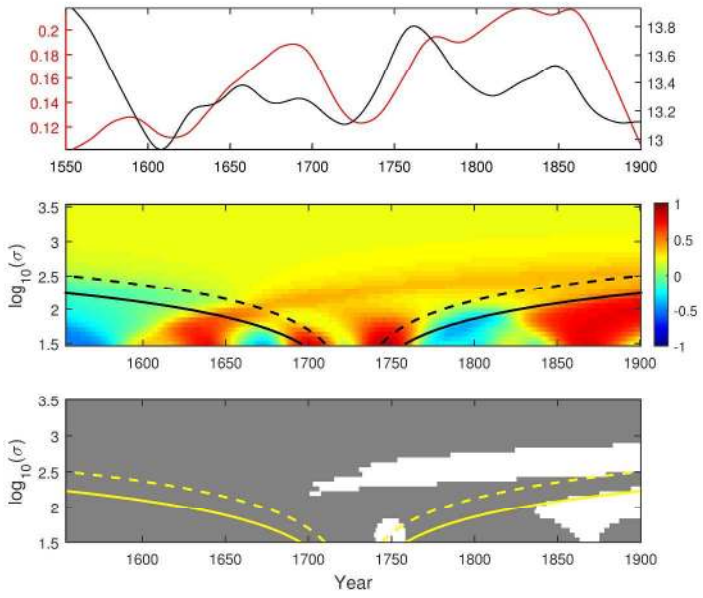

Fig. 6. The results of the scale-correlation analysis of smoothed fire synchrony vs. summer temperature reconstruction. The upper panel shows the smoothed time series analyzed (posterior mean values; red = fire synchrony, black = summer temperature). The middle panel shows the correlation map (posterior mean values), and the lower panel the results of the credibility analysis for the correlation map (white = credibly positive correlation, gray = correlation not credible). The horizontal space between the solid lines in the two lower panels indicate the width of a centrally positioned kernel and the dashed lines similarly indicate the width of the interval where the kernel height has decreased to 50% of its maximum value.

279x361mm (300 x 300 DPI)

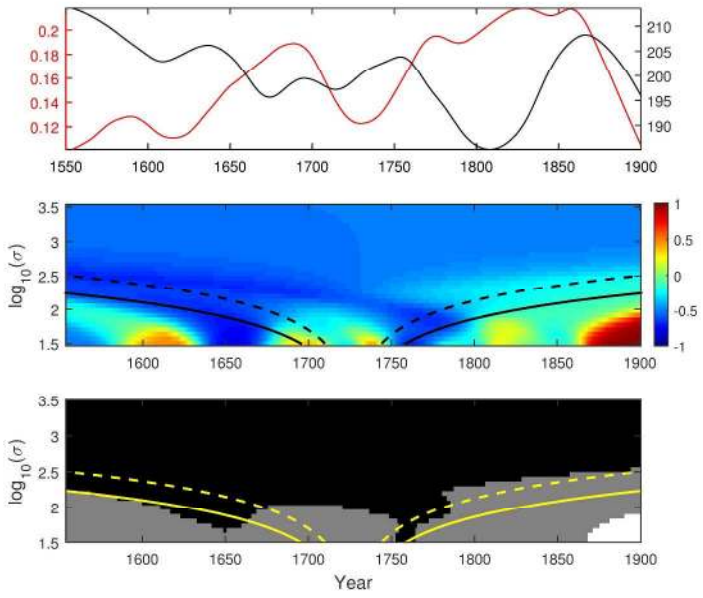

Fig. 7. The results of the scale-correlation analysis of smoothed fire synchrony vs. summer precipitation reconstruction. The upper panel shows the smoothed time series analyzed (posterior mean values; red = fire synchrony, black = summer precipitation). The middle panel shows the correlation map (posterior mean values), and the lower panel the results of the credibility analysis for the correlation map (white = credibly positive correlation, gray = correlation not credible, black = credibly negative correlation). Interpretation otherwise as in Fig. 6.

279x361mm (300 x 300 DPI)

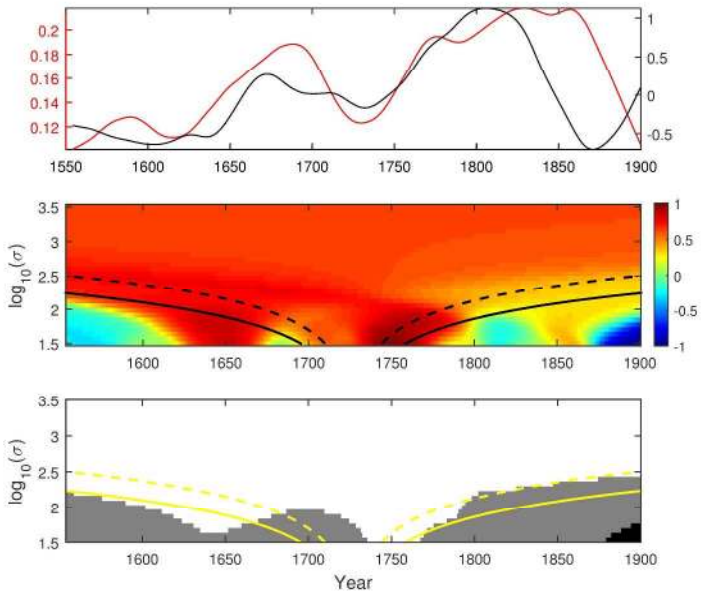

Fig. 8. The results of the scale-correlation analysis of smoothed fire synchrony vs. summer drought index reconstruction. The upper panel shows the smoothed time series analyzed (posterior mean values; red = fire synchrony, black = summer drought index). The middle panel shows the correlation map (posterior mean values), and the lower panel the results of the credibility analysis for the correlation map. Interpretation otherwise as in Fig. 6.

279x361mm (300 x 300 DPI)